THE JOURNAL OF BIOLOGICAL CHEMISTRY Vol. 276, No. 46, Issue of November 16, pp. 42801–42806, 2001
Printed in U.S.A.

Optimization of Receptor-G Protein Coupling by Bilayer Lipid Composition I

KINETICS OF RHODOPSIN-TRANSDUCIN BINDING*

Received for publication, June 21, 2001, and in revised form, August 22, 2001
Published, JBC Papers in Press, September 5, 2001, DOI 10.1074/jbc.M105772200

Drake C. Mitchell, Shui-Lin Niu, and Burton J. Litman‡

From the Section of Fluorescence Studies, Laboratory of Membrane Biochemistry and Biophysics, National Institute on Alcohol Abuse and Alcoholism, Rockville, Maryland 20852

The role of membrane composition in modulating the rate of G protein-receptor complex formation was examined using rhodopsin and transducin (G_t) as a model system. Metarhodopsin II (MII) and MII-G_t complex formation rates were measured, in the absence of GTP, via flash photolysis for rhodopsin reconstituted in 1-stearoyl-2-oleoyl-*sn*-glycero-3-phosphocholine (18:0,18:1PC) and 1-stearoyl-2-docosahexaenoyl-*sn*-glycero-3-phosphocholine (18:0,22:6PC) bilayers, with and without 30 mol% cholesterol. Variation in bilayer lipid composition altered the lifetime of MII-G_t formation to a greater extent than the lifetime of MII. MII-G_t formation was fastest in 18:0,22:6PC and slowest in 18:0,18:1PC/30 mol% cholesterol. At 37 °C and a G_t to photolyzed rhodopsin ratio of 1:1 in 18:0,22:6PC bilayers, MII-G_t formed with a lifetime of 0.6 ± 0.06 ms, which was not significantly different from the lifetime for MII formation. Incorporation of 30 mol% cholesterol slowed the rate of MII-G_t complex formation by about 400% in 18:0,18:1PC, but by less than 25% in 18:0,22:6PC bilayers. In 18:0,22:6PC, with or without cholesterol, MII-G_t formed rapidly after MII formed. In contrast, cholesterol in 18:0,18:1PC induced a considerable lag time in MII-G_t formation after MII formed. These results demonstrate that membrane composition is a critical factor in determining the temporal response of a G protein-coupled signaling system.

In G protein-coupled signaling pathways, the stimulus is passed from the receptor to a G protein and subsequently, to an effector enzyme. The number of G protein-coupled signaling pathways has grown tremendously in the past 10 years, and now includes sensory pathways associated with vision, olfaction, taste, and receptors for dopamine, serotonin, γ-aminobutyric acid, and histamine. Much of the basic information about G protein-coupled signaling pathways was obtained from work on the visual system (1, 2), and it is the only G protein-coupled pathway for which there are three-dimensional structures for both the receptor, rhodopsin (3), and G protein, transducin (G_t)[1] (4). A unique aspect of the visual system is the rapid rate of G protein activation. Recent biochemical measurements establish that G_t activation by rhodopsin occurs about 100 times faster than the activation of other G proteins (5). Two properties are believed to be responsible for this rapid rate of G_t activation: 1) the high concentration of G_t on the surface of the rod outer segment disc membrane and 2) the low degree of acyl chain packing order in the disc membrane, resulting from the high levels of phospholipid acyl chain polyunsaturation (5). Recent experiments with whole rod cells from transgenic mice that expressed half the normal amount of rhodopsin establish that the rate of phototransduction in the rod cell is determined by protein diffusion in the disc membrane (6).

Within a few milliseconds of photon absorption, a metastable equilibrium is established between two conformational states of photoexcited rhodopsin, MI and MII (7). MII is the conformation of photoisomerized rhodopsin that binds and activates G_t (8–10). G_t is bound to the membrane by a combination of electrostatic forces (11) and hydrophobic forces associated with a farnesyl group on the γ subunit of G_t (12, 13). The binding interaction between rhodopsin and G_t has been examined in some detail (for reviews, see Refs. 14 and 15). Binding of G_t by MII catalyzes the exchange of GDP for GTP, and the visual "signal" is carried from rhodopsin to the effector enzyme, a cGMP-specific phosphodiesterase. The activated phosphodiesterase catalyzes the hydrolysis of cGMP, which triggers the closure of cGMP gated Na^+/Ca^{2+} channels leading to the hyperpolarization of the rod outer segment (ROS) plasma membrane and the visual response. In the absence of GTP, the MII-G_t complex is stable and has the same absorption spectrum as unbound MII. In the outer segment of the human rod cell there are about 10 rhodopsin molecules for every G_t molecule. However, during normal physiological function, only ~1 rhodopsin of every 100,000 is photoisomerized and active at any one time. Consequently, the rate of MII-G_t complex formation is governed by a two-dimensional, diffusion-controlled search in the plane of the disc membrane of G_t for photoactivated rhodopsin, in its MII conformational state (6).

Previous studies in this laboratory (16) and others (17, 18) demonstrate that the equilibrium concentration of MII is increased by the presence of phospholipids with one or more 22:6*n*-3 acyl chains. An important aspect of visual signal transduction is rapid response, and studies on rhesus monkeys show that electroretinagram b-wave implicit times (19) and a-wave

* The costs of publication of this article were defrayed in part by the payment of page charges. This article must therefore be hereby marked "*advertisement*" in accordance with 18 U.S.C. Section 1734 solely to indicate this fact.

‡ To whom correspondence should be addressed: Section of Fluorescence Studies, Laboratory of Membrane Biochemistry and Biophysics, National Institute on Alcohol Abuse and Alcoholism, Park 5, Rm. 158, 12420 Parklawn Dr., Rockville, MD 20852. Tel.: 301-594-3608; Fax: 301-594-0035; E-mail: litman@helix.nih.gov.

[1] The abbreviations used are: G_t, transducin; 22:6*n*-3, docosahexaenoic acid, or DHA; 22:5*n*-6, docosapentaenoic acid, or DPA; 18:0,22:6PC, 1-stearoyl-2-docosahexaenoyl-*sn*-glycero-3-phosphocholine; 18:0,18:1PC, 1-stearoyl-2-oleoyl-*sn*-glycero-3-phosphocholine; MI, metarhodopsin I; MII, metarhodopsin II; ROS, rod outer segment; $\langle\tau\rangle_{MII}$, average lifetime of metarhodopsin II formation; $\langle\tau\rangle$MII-G_t, average lifetime of MII-G_t complex formation; K_{eq}^{-G}, MI-MII equilibrium constant in the absence of G_t; K_{eq}^{+G}, apparent MI-MII equilibrium constant in the presence of G_t; TBS, Tris-buffered saline; GTPγS, guanosine 5′-3-*O*-(thio)triphosphate.

implicit times[2] are delayed in *n*-3-deficient animals. Studies on human infants show that light-adapted oscillatory potentials are delayed in infants fed standard infant formula without 22:6*n*-3 relative to infants fed 22:6*n*-3-supplemented formula (20). The present study was undertaken to determine the effects of 22:6*n*-3 and cholesterol on the kinetics of the first two steps in visual signal transduction, which are the formation of MII and the binding of G_t to MII. The latter process represents the first stage in signal amplification in the visual transduction pathway.

EXPERIMENTAL PROCEDURES

Sample Preparation—Phospholipids 18:0,18:1PC and 18:0,22:6PC were purchased from Avanti Polar Lipids Inc. (Alabaster, AL), and their purity was ascertained by high performance liquid chromatography. Cholesterol was purchased from Calbiochem (La Jolla, CA). All preparation of phospholipids was carried out in an argon-filled glove box and in thoroughly degassed buffers because of the susceptibility to oxidation of polyunsaturated phospholipids. ROS were isolated from frozen retinas (James and Wanda Lawson, Lincoln, NE) as described previously (21). ROS was solubilized in octyl glucoside, and rhodopsin was purified on a concanavalin A affinity column (22). Large unilamellar vesicles containing rhodopsin at a ratio of 1 rhodopsin to 100 phospholipids were prepared using the rapid dilution technique (23). Following dialysis to remove detergent, all vesicle preparations were suspended in pH 7.5 Tris basal salt (TBS) buffer consisting of 10 mM Tris, 60 mM NaCl, 30 mM KCl, 50 μM diethylenetriamine pentaacetic acid. G_t was prepared from ROS as a hypotonic extract (24), the activity level was determined by a binding assay using ^{35}S-labeled GTPγS (25), and stored in pH 7.5 TBS buffer with 30% glycerol at −20 °C for no longer than 2 weeks. The phospholipid, cholesterol, and rhodopsin content of each reconstituted vesicle preparation were determined by independent phosphate (26), cholesterol (Waco Chemicals USA, Inc., Richmond, VA), and ΔA_{500} assays, respectively. Samples for flash photolysis measurements were prepared by diluting concentrated, reconstituted vesicle stocks with pH 7.5 TBS buffer, dividing the solution in half, and adding concentrated G_t to one half and an identical amount of G_t buffer to the other half. Samples were then incubated for 4 h on ice to ensure binding of G_t to the bilayer (24). Final concentrations were 7.5 μM rhodopsin and 0.5–1.5 μM G_t.

Flash Photolysis Measurements—Kinetics of MII and MII 158 G_t formation were assessed by measuring the transient absorption at 380 nm using a flash photolysis system constructed in the laboratory (27) with the following modifications. Excitation was provided by a high pressure flash lamp (E.G. & G., pulse width = 1μs) filtered with a broad (± 25 nm) bandpass filter centered at 500 nm. The current from a thermoelectrically cooled photomultiplier tube (R928, Hamamatsu) was passed to a low noise current amplifier (Stanford Research). The amplifier output voltage was acquired at 2–10 μs/point by a 1.25-MHz., 12-bit analog-to-digital converter (National Instruments) installed in a PC.

Data Analysis—The detailed kinetics of MII formation were extracted from the changes in absorbance observed at 380 nm in the absence of G_t via analysis in terms of the microscopic rate constants of the square (28) and branched (27) photoreaction models shown in Fig. 1. The observed absorbance increase at 380 nm was directly analyzed in terms of the microscopic rate constants of the two models using NONLIN (29) with subroutines specifying each model written by the authors.

The dilution reconstitution procedure produces rhodopsin-containing vesicles with half of the rhodopsin oriented with its cytoplasmic face external to the vesicle and half with the cytoplasmic face internal to the vesicle (23). G_t that has been added to the vesicle suspension can only interact with half of the rhodopsin; thus, the absorbance change observed in the presence of G_t is the result of three distinct species: MII_{inside}, $MII_{outside}$, and MII-G_t. To isolate the absorbance increase caused by formation of MII-G_t, it is necessary to remove the contributions resulting from MII_{inside} and $MII_{outside}$. The absorbance change recorded in the absence of G_t was multiplied by the following scaling factor and subtracted from the absorbance change recorded in the presence of G_t.

$$\text{Scaling factor} = [(K_{eq}^{-G} + 1)/(K_{eq}^{+G} + 1) + 1]/2 \qquad \text{(Eq. 1)}$$

[2] B. G. Jeffrey, D. C. Mitchell, M. Neuringer, and R. A. Gibson, submitted for publication.

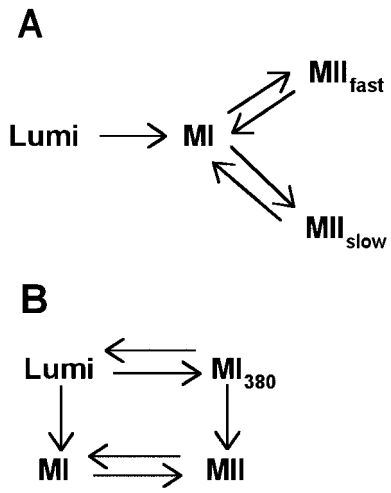

FIG. 1. **Microscopic rate models of the rhodopsin photointermediate cascade from lumirhodopsin to MI-MII.** *A*, branched model (27); *B*, square model (28).

K_{eq}^{-G} and K_{eq}^{+G} are the MI-MII equilibrium constants measured in the absence and presence of G_t, respectively, and were determined from equilibrium measurements on the same samples used for the kinetic measurements (30). Absorbance increases at 380 nm observed in the presence of G_t were analyzed with the two microscopic photoreaction models shown in Fig. 1 plus a sum-of-two exponentials process for the binding of G_t to MII.

RESULTS

The rate of formation of MII and MII-G_t complex in 18:0,22:6PC and 18:0,18:1PC with and without 30 mol% cholesterol was measured by flash photolysis. The flash-induced increase in absorbance at 380 nm, near the absorbance maximum for MII, was monitored from 20 μs to several hundred ms. For samples containing G_t, it was necessary to separate the rate of MII formation from that of the MII-G_t complex by characterizing the kinetics of MII formation observed in the absence of G_t. The increase in absorbance corresponding to the formation of MII was analyzed using the two microscopic photoreaction models shown in Fig. 1, which characterize the portion of the rhodopsin photoreaction cascade from the decay of lumirhodopsin to the formation of MII. An example of the flash-induced increase in absorbance at 380 nm for rhodopsin in 18:0,22:6PC/30 mol% cholesterol with and without added G_t at 37 °C is shown in Fig. 2. The results of the analysis for the G_t-free sample using the branched model (Ref. 27; Fig. 2*A*) and the square model (Ref. 28; Fig. 2*B*) demonstrate the difference between these two models. In the branched model, both MII_{fast} and MII_{slow} are present at equilibrium; thus, the MI-MII equilibrium for this model is calculated according to $K_{eq} = (MII_{fast} + MII_{slow})/MI$. The two models produced values of K_{eq} for the MI-MII equilibrium that agreed with each other, as shown by the similar amplitudes for both MI and total MII for both models. The significant difference between the two photoreaction models is the manner in which they account for the most rapidly appearing species with an absorbance at 380 nm. For the branched model, the most rapidly forming species is MII_{fast} (*dashed curve*, Fig. 2*A*), which rises to a maximum at ~ 200 μs and decays to a level such that it constitutes ~25% of total MII at equilibrium. In the square model, the most rapidly forming species with an absorbance at 380 nm is MI_{380} (*dashed curve*, Fig. 2*B*), which reaches a maximum at ~200 μs and then decays to zero by 6 ms. The decay of MI_{380} to zero results in the time course for formation of total MII being shifted to the right for the square model (*solid curve*, Fig. 2*B*) relative to the branched model (*solid curve*, Fig. 2*A*). An exponential rise to a plateau is characterized by the lifetime, τ, denoting the time

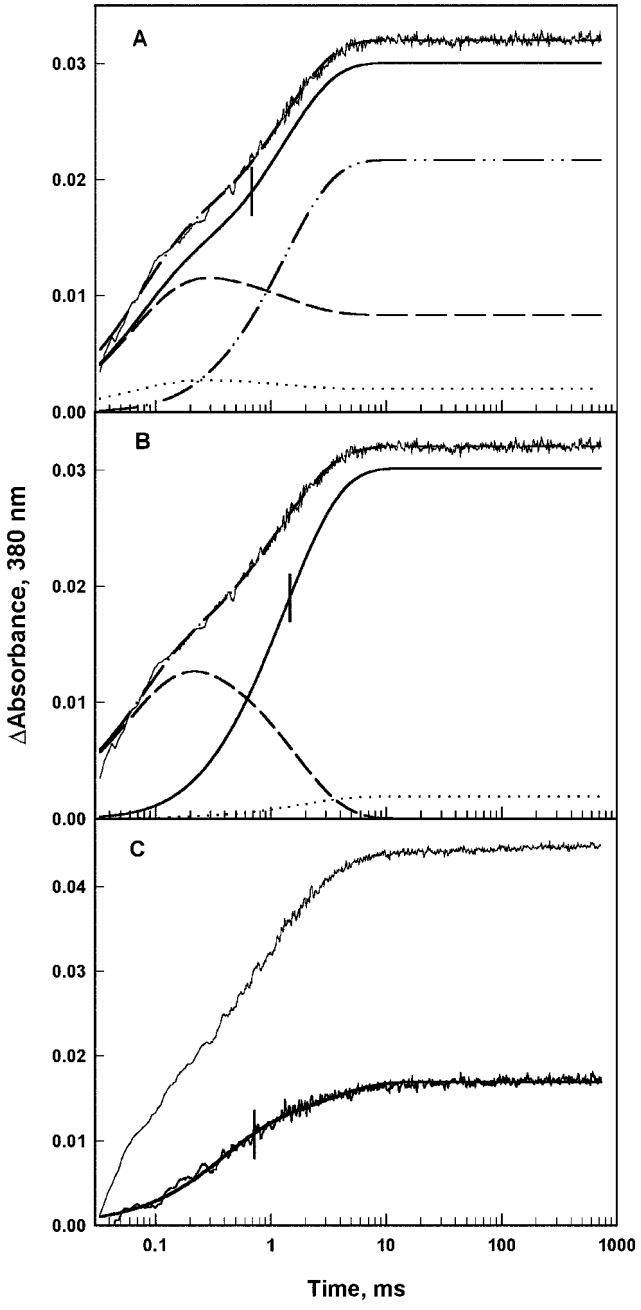

FIG. 2. **The two microscopic rate models in Fig. 1 lead to different lifetimes for MII formation at 37 °C.** *A*, example of analysis with branched model. – – –, MII_{fast}; – · · – · · –, MII_{slow}; · · ·, contribution resulting from MI; ——, total MII; – · – · –, total fit. *B*, example of analysis with square model. – – –, MI_{380}; · · ·, contribution resulting from MI; ——, MII; – · – · –, total fit. *C*, *upper curve*, increase in absorbance at 380 nm at 37 °C in the presence of 1.5 μM G_t; *lower curve*, results of subtracting the kinetic trace observed in the absence of G_t (shown in *panels A* and *B*) after scaling according to Equation 1.

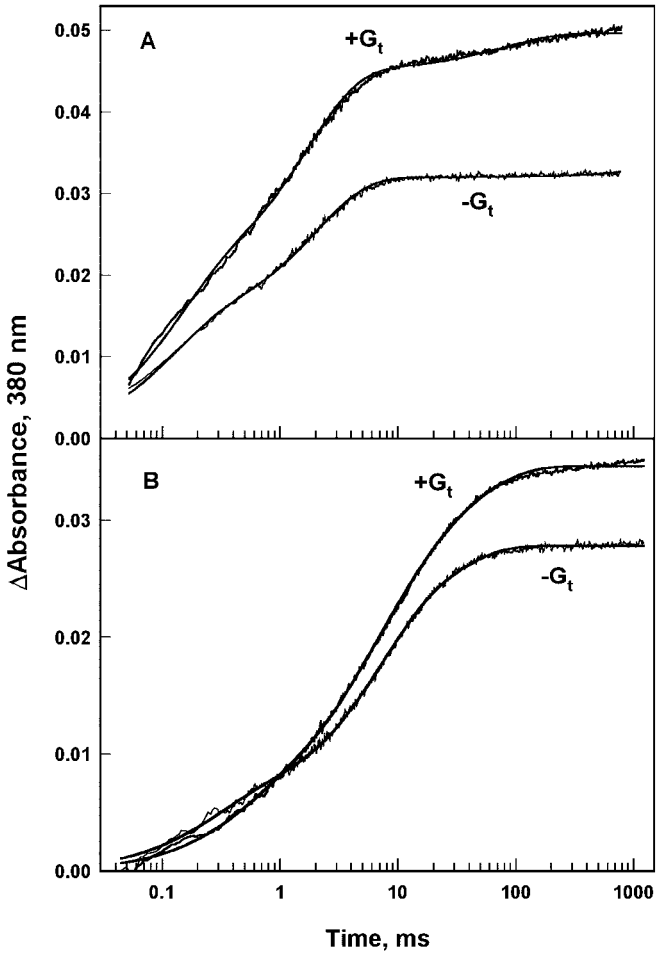

FIG. 3. **At 37 °C, the MII-G_t complex forms with a lifetime comparable with that for MII, whereas at 20 °C, the MII-G_t complex forms significantly slower than MII.** *A*, rhodopsin in 18:0,18:1PC with and without G_t at 37 °C. *B*, rhodopsin in 18:0,18:1PC with and without G_t at 20 °C.

required to rise to within $(1 - 1/e)$ of the final, equilibrium value. The *vertical mark* in the *solid curves* in Fig. 2 (*A* and *B*) denotes τ for total MII. For the branched model this occurs 0.68 ms after flash, and for the square model it occurs 1.47 ms after flash.

The significance of the 0.79-ms difference in the rate of formation of MII for the two models is illustrated by the analysis of the flash-induced kinetics in the presence of G_t, shown in Fig. 2*C*. The *upper curve* in Fig. 2*C* was obtained for a sample identical to the one shown in Fig. 2 (*A* and *B*), except that it contains 1 μM G_t. The *lower curve* in Fig. 2*C* is the isolated formation of the MII-G_t complex, as determined by an empirical separation of the raw data. The separation was accomplished by scaling the transient recorded without G_t according to Equation 1 and subtracting it from the transient observed in the presence of G_t. Inspection of this curve shows that it rises very rapidly, and the *hash mark* denotes the time, 0.74 ms, when it reaches to within $(1 - 1/e)$ of its equilibrium value. Thus, the lifetime for MII formation, according to the square model, is greater than the lifetime for the MII-G_t complex formation. This physically improbable situation is simply a result of the provision in the square model that the most rapidly forming species at 380 nm is a MI species that decays to zero at equilibrium. In the branched model, the most rapidly forming species at 380 nm is a kinetically distinct form of MII. As a result, formation of total MII, according to the branched model, is approximately coincident with formation of the MII-G_t complex. The analysis and comparisons presented in Fig. 2 make it clear that at 37 °C the fastest component appearing at 380 nm must correspond to a "normal" MII species that is capable of binding G_t. Because of the consistency generated for the kinetics of the MII and MII-G_t formation, the branched model for the Lumi-MI-MII portion of the rhodopsin photoreaction cascade was employed in all analysis.

In the absence of G_t, all kinetic data were well described by the branched model (Fig. 1), as shown by the smooth curves through the data obtained in the absence of G_t, as shown in Fig. 3. The flash-induced increase in equilibrium absorbance at 380

nm is proportional to the MI-MII equilibrium constant, K_{eq}^{-G}. The values of K_{eq}^{-G} calculated from the branched model agreed with those determined from equilibrium difference spectra obtained for the same samples (30). Agreement between the values of K_{eq}^{-G} determined from equilibrium measurements and from analysis of kinetic data with the branched model was reported previously (31, 32). In the presence of G_t, all kinetic data were well described by using the solution to the branched model obtained in the absence of G_t, rescaled according to Equation 1, plus the sum of two exponential terms, as shown by the smooth curves through the kinetic absorbance changes acquired in the presence of G_t (Fig. 3).

The *two pairs* of *curves* in Fig. 3 demonstrate one of the fundamental differences between the kinetic processes observed at 37 °C and those observed at 20 °C. The two kinetic traces observed at 37 °C (Fig. 3*A*) diverge within ~100 μs of the activating flash, demonstrating the rapid formation of the MII-G_t complex. In contrast, the two kinetic traces observed at 20 °C (Fig. 3*B*), do not diverge until 2 or 3 ms after flash. This difference demonstrates that, at 37 °C, the MII-G_t complex forms very quickly after MII formation, whereas, at 20 °C, there is a lag time in the formation of the MII-G_t complex relative to MII.

The increase in absorbance at 380 nm was measured in the absence and presence of G_t at physiological temperature for rhodopsin in vesicles with four different bilayer compositions: 18:0,22:6PC and 18:0,18:1PC, with and without 30 mol% cholesterol. Changes in phospholipid acyl chain composition and cholesterol altered the kinetics of both MII formation (Fig. 4*A*) and MII-G_t complex formation (Fig. 4*B*). The data in each panel in Fig. 4 have been scaled to the same maximum change in absorbance to facilitate comparison of the differences in kinetics. Comparison of the curves in *panels A* and *B* of Fig. 4 show that, whereas both decreased acyl chain unsaturation and increased bilayer cholesterol delay the formation of MII, variation in these parameters cause an even greater delay in the formation of the MII-G_t complex.

Complete analysis of the kinetic data acquired at 37 °C, summarized in Fig. 5, shows that cholesterol has relatively little effect on the kinetics of either MII or MII-G_t formation in a bilayer consisting of 18:0,22:6PC. This is consistent with a number of measurements that show that cholesterol has its smallest effect on bilayer properties in bilayers that contain 22:6*n*-3 acyl chains (33). In contrast, in an 18:0,18:1PC bilayer, cholesterol increases the time required for MII formation by 50%, and the time required for MII-G_t formation by 400%. Reducing *sn*-2 acyl chain unsaturation from 22:6 to 18:1 doubles the time required for both MII formation and MII-G_t formation. At physiological temperature, the rates of MII-G_t complex formation approach those of MII formation in all bilayer compositions examined, with the exception of 18:0,18:1PC/30 mol% cholesterol, as shown in Fig. 5.

To isolate the effects of bilayer composition on the lateral diffusion process that leads to formation of the MII-G_t complex, it is informative to compare the lifetimes for MII formation and MII-G_t complex formation. Comparison of the ratio of the average lifetimes, $\langle\tau\rangle_{\text{MII-G}_{t/(?)}\text{MII}}$, eliminates the effect of delayed MII formation on the diffusional search process. At physiological temperature, MII formation and MII-G_t complex formation are nearly coincident in 18:0,22:6PC, even in the presence of 30 mol% cholesterol, as shown in Table I. Because MII cannot react with G_t any faster than it is formed from MI, the rate of formation of MII-G_t complex in 18:0,22:6PC appears to be maximal. In 18:0,22:6PC, the rate of MII-G_t complex formation, which is limited by lateral diffusion, is only slightly altered by the presence of 30 mol% cholesterol, further suggesting that

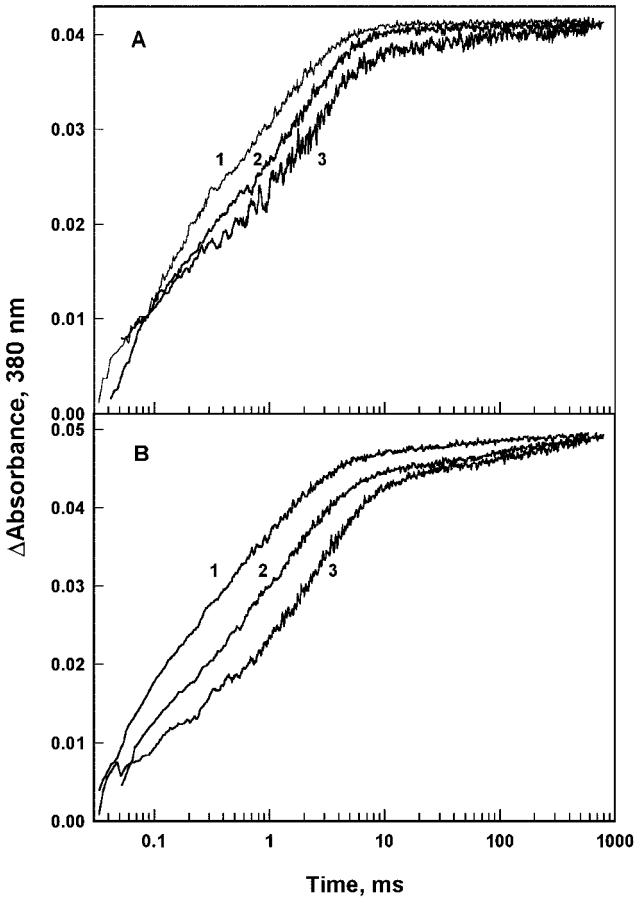

FIG. 4. **Bilayer composition alters the kinetics of the flash-induced absorbance change observed at 380 nm, 37 °C.** Data in both panels were rescaled to demonstrate the differences in kinetics. *A*, absorption kinetics observed in the absence of G_t: *trace 1*, rhodopsin in 18:0,22:6PC; *trace 2*, rhodopsin in 18:0,18:1PC; *trace 3*, rhodopsin in 18:0,18:1/30 mol% cholesterol. *B*, absorption kinetics observed in the presence of 1.5 μM G_t: *trace 1*, rhodopsin in 18:0,22:6PC; *trace 2*, rhodopsin in 18:0,18:1PC; *trace 3*, rhodopsin in 18:0,18:1/30 mol% cholesterol.

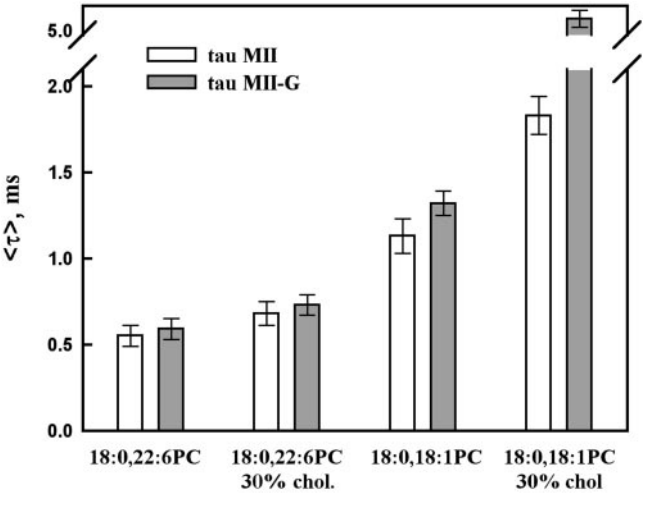

FIG. 5. **Summary of the effects of phospholipid acyl chain composition and bilayer cholesterol content on the average lifetimes of MII and MII-G_t formation at 37 °C.**

18:0,22:6PC has the optimum acyl chain composition for rapid formation of receptor-G protein complex. In 18:0,18:1PC, the addition of 30 mol% cholesterol increases the lifetime ratio by about a factor of 2.5, demonstrating the sharp reduction in the

TABLE I
Average lifetimes (ms) for MII and MII-G_t complex formation and their ratio at 20 °C and 37 °C

	20 °C			37 °C		
	$\langle\tau\rangle_{MII}$	$\langle\tau\rangle_{MII\text{-}Gt}$	$\langle\tau\rangle_{MII\text{-}Gt}/\langle\tau\rangle_{MII}$	$\langle\tau\rangle_{MII}$	$\langle\tau\rangle_{MII\text{-}Gt}$	$\langle\tau\rangle_{MII\text{-}Gt}/\langle\tau\rangle_{MII}$
18:0,22:6PC	10.1 ± 0.4	13.9 ± 0.3	1.4 ± 0.1	0.55 ± 0.06	0.59 ± 0.06	1.1 ± 0.2
18:0,22:6PC/30 mol% cholesterol	10.6 ± 0.2	15.9 ± 0.3	1.5 ± 0.1	0.68 ± 0.07	0.73 ± 0.06	1.1 ± 0.2
18:0,18:1PC	7.6 ± 0.2	22.2 ± 0.8	2.9 ± 0.2	1.12 ± 0.1	1.32 ± 0.07	1.2 ± 0.2
18:0,18:1PC/30 mol% cholesterol	15.7 ± 0.4	56.8 ± 2.0	3.6 ± 0.2	1.83 ± 0.11	5.3 ± 0.2	2.9 ± 0.3

rate of lateral diffusion caused by cholesterol in a bilayer with a low level of unsaturation. In 18:0,18:1PC, the lifetime ratio is about the same as in 18:0,22:6PC, but both $\langle\tau\rangle_{MII}$ and $\langle\tau\rangle_{MII\text{-}G}$ are approximately doubled, indicative of the slower kinetics caused by reduced acyl chain unsaturation at the *sn*-2 position.

At 20 °C the rates of MII and MII-G_t formation in bilayers were slower than those at 37 °C. The greatest effect of bilayer composition was on the lifetime for diffusion-dependent MII-G_t complex formation, as shown in Table I. The MII-G_t complex forms at about the same rate in bilayers consisting of 18:0,22:6PC and 18:0,22:6PC/30 mol% cholesterol, but forms much slower in a bilayer consisting of 18:0,18:1PC/30 mol% cholesterol. In both pure phospholipid bilayers and cholesterol-containing bilayers, the MII-G_t complex formed fastest in 18:0,22:6PC, as shown in Table I. In pure 18:0,18:1PC, the MII-G_t complex formed 60% slower than in 18:0,22:6PC, and the addition of 30 mol% cholesterol slowed MII-G_t complex formation by a factor of 2.5 in 18:0,18:1PC, whereas it had relatively little effect in 18:0,22:6PC. These differences suggest that a high level of polyunsaturation at the *sn*-2 position increases the rate of G_t lateral diffusion.

DISCUSSION

The bilayer compositions examined in this study produced changes in the rates of formation of both MII and MII-G_t complex, demonstrating that the diffusion of receptor and G protein are sensitive to the lipid composition of the membrane. G_t is anchored to the membrane by an isoprenoid moiety; thus, the effects of bilayer composition on G_t lateral diffusion are likely to be similar to those observed for phospholipid lateral diffusion. The present results are consistent with changes in the rate of lateral diffusion of fluorescent phospholipids caused by changes in bilayer cholesterol (34) and changes in polyunsaturated acyl chain oxidation (35). These two studies reported a positive correlation between slower lateral diffusion and more ordered acyl chain packing. Previous studies demonstrate that increased phospholipid acyl chain unsaturation leads to more disordered acyl chain packing and increased bilayer free volume (36). The present results are also in agreement with a detailed analysis of lateral diffusion in di14:0PC/cholesterol bilayers that determined that cholesterol slows phospholipid lateral diffusion by decreasing phospholipid acyl chain packing free volume (37).

A unique feature of this study is the comparison of the kinetics of the unimolecular MI-to-MII reaction and the diffusion-dependent MII-G_t at physiological temperature and at a reduced temperature. The results presented in Fig. 3 and summarized in Table I demonstrate that these two kinetic processes are slowed to different degrees by reduced temperature. In a bilayer consisting of 18:0,18:1PC, at 37 °C, the lifetime for MII-G_t formation is only 20% greater than the lifetime for MII formation. However, at 20 °C, MII-G_t formation trails MII formation by a factor of 3. The implication of this difference is that studies of MII-G_t binding must be carried out at physiological temperature if the ultimate goal of the investigation is provide an explanation for processes observed *in vivo*.

It is noteworthy that, among the bilayer compositions examined, the two compositions that most closely resemble the native ROS disc membrane are 18:0,22:6PC with and without 30 mol% cholesterol. Like the native membrane, 50% of the acyl chains in these bilayers are 22:6*n*-3, and the basal disc membranes contain 30 mol% cholesterol (38), and the predominant acyl chain configuration of 22:6-containing phospholipids in the ROS disc membrane is *sn*-1 saturated, *sn*-2 22:6*n*-3 (39). The results presented here suggest that the delays in electroretinagram response observed in dietary *n*-3 deficiency[2] (19, 20) could be partially the result of a slower rate of MII-G_t formation in the absence of 22:6*n*-3 phospholipid acyl chains. At physiological temperature and the conditions of our measurements, MII-G_t complex formed twice as slowly in 18:0,18:1PC relative to 18:0,22:6PC. The measurement conditions differ from those found *in vivo* in several respects. The two most significant differences are the low level of rhodopsin stimulation *in vivo* and the large contrast in acyl chain composition between 18:0,18:1PC and 18:0,22:6PC. In the measurements reported here, 15% of the rhodopsin was bleached, resulting in an average distance between MII molecules of 15 nm. The physiological range of rod cell function involves activation of about 1 rhodopsin of every 100,000, resulting in an average distance between MII molecules of about 1000 nm. Thus, the experimental conditions employed in the present study would tend to lessen the effects of altered receptor and/or G protein lateral diffusion on the rate MII-G_t formation relative to what would be observed under physiological conditions. The comparison of 18:1 and 22:6 at the *sn*-2 position is a greater alteration than that produced by dietary *n*-3 fatty acid deficiency, which generally leads to replacement of 22:6*n*-3 with 22:5*n*-6 (40). Thus, the bilayer compositions examined in the present study exaggerate the differences in membrane composition produced by dietary *n*-3 deficiency. The increase in $\langle\tau\rangle_{MII\text{-}G}$ caused by exchanging 22:6 for 18:1 at the *sn*-2 position, corresponds to a 50% reduction in the rate of binding of G_t to MII. The initial rising phase of the rod cell photoresponse is a parabolic function of time and a linear function of the rate of activation of phosphodiesterase catalytic subunits per unit time (5). Biochemical analysis shows that the rates of G_t activation and phosphodiesterase catalytic subunit activation are approximately equal (5). Assuming that the rates of G_t binding and G_t activation are similar, this means that a reduction in the rate of MII-G_t complex formation by 10% will delay the rod cell photoresponse by 5%. We report a 50% reduction in the rate of MII-G_t complex formation, under conditions that minimize the effects of lateral diffusion relative to physiological conditions. These results indicate that the effect of membrane composition on the rates of rhodopsin and/or G_t lateral diffusion would be sufficient to account for the 5% delay in a-wave implicit time activity observed in dietary *n*-3 deficiency.[2]

Since the classical photoreaction cascade of Lumi → Meta I → Meta II was introduced by Wald and co-workers (7), a number of additional photointermediates on the microsecond to millisecond timescale have been proposed based on observed kinetic complexity (27, 28), proton motions (41), effects of pH (42, 43), and interaction with G_t that requires GTP (44). Several investigations have determined that the full complexity of the transitions between photointermediates occurring on the

MI-to-MII time scale become most apparent when examined at physiological temperature (27, 45). However, no previous study has examined the interaction of G_t with MII, or any other 380 nm-absorbing species at 37 °C. The data and analysis presented in Fig. 2 provide strong evidence that the most rapidly forming photointermediate with an absorbance at 380 nm is part of the classical MI-MII equilibrium and binds G_t. The measurements presented in this study do not address issues raised by other investigations such as the effect of pH, proton uptake, or possible effects of GTP on the MI-to-MII transition. All measurements were made in the absence of GTP, a condition that leads to the formation of a G_t-MI_b complex in measurements at −35 °C (44). However, the measurements reported here for samples at 37 °C showed no evidence for binding of G_t to a state other than MII.

The visual signal transduction pathway has been optimized by evolution to be one of the most rapid and highly amplified signal transduction pathways in the human body. The present results demonstrate that the lipid composition of the rod outer segment disc membrane makes a significant contribution to the optimal kinetic functioning of this prototypical G protein-coupled pathway. The excitable membranes of the nervous system all contain high levels of phospholipids with polyunsaturated acyl chains, thus it is expected that the results presented here will be applicable to G protein-coupled systems associated with neurotransmitters, taste, and olfaction and should be generally applicable to other members in the G protein-coupled superfamily.

REFERENCES

1. Hargrave, P. A., and McDowell, J. H. (1992) *FASEB J.* **6,** 2323–2331
2. Sakmar, T. P. (1998) *Prog. Nucleic Acid Res. Mol. Biol.* **59,** 1–34
3. Palczewski, K., Kumasaka, T., Hori, T., Behnke, C. A., Motoshima, H., Fox, B. A., Le, T., I, Teller, D. C., Okada, T., Stenkamp, R. E., Yamamoto, M., and Miyano, M. (2000) *Science* **289,** 739–745
4. Lambright, D. G., Sondek, J., Bohm, A., Skiba, N. P., Hamm, H. E., and Sigler, P. B. (1996) *Nature* **379,** 311–319
5. Leskov, I. B., Klenchin, V. A., Handy, J. W., Whitlock, G. G., Govardovskii, V. I., Bownds, M. D., Lamb, T. D., Pugh, E. N., and Arshavsky, V. Y. (2000) *Neuron* **27,** 525–537
6. Calvert, P. D., Govardovskii, V. I., Krasnoperova, N., Anderson, R. E., Lem, J., and Makino, C. L. (2001) *Nature* **411,** 90–94
7. Mathews, R., Hubbard, R., Brown, P., and Wald, G. (1963) *J. Gen. Physiol.* **47,** 215–222
8. Kibelbek, J., Mitchell, D. C., Beach, J. M., and Litman, B. J. (1991) *Biochemistry* **30,** 6761–6768
9. Emeis, D., Kuhn, H., Reichert, J., and Hofmann, K. P. (1982) *FEBS Lett.* **143,** 29–34
10. Bennett, N., Michel-Villaz, M., and Kuhn, H. (1982) *Eur. J. Biochem.* **127,** 97–103
11. Seitz, H. R., Heck, M., Hofmann, K. P., Alt, T., Pellaud, J., and Seelig, A. (1999) *Biochemistry* **38,** 7950–7960
12. Matsuda, T., Takao, T., Shimonishi, Y., Murata, M., Asano, T., Yoshizawa, T., and Fukada, Y. (1994) *J. Biol. Chem.* **269,** 30358–30363
13. Kisselev, O. G., Ermolaeva, M. V., and Gautam, N. (1994) *J. Biol. Chem.* **269,** 21399–21402
14. Hargrave, P. A., Hamm, H. E., and Hofmann, K. P. (1993) *Bioessays* **15,** 43–50
15. Bourne, H. R. (1997) *Curr. Opin. Cell Biol.* **9,** 134–142
16. Litman, B. J., and Mitchell, D. C. (1996) *Lipids* **31,** (suppl.) S193–S197
17. Brown, M. F. (1994) *Chem. Phys. Lipids* **73,** 159–180
18. O'Brien, D. F., Costa, L. F., and Ott, R. A. (1977) *Biochemistry* **16,** 1295–1303
19. Neuringer, M., Connor, W. E., Lin, D. S., Barstad, L., and Luck, S. (1986) *Proc. Natl. Acad. Sci. U. S. A.* **83,** 4021–4025
20. Birch, D. G., Birch, E. E., Hoffman, D. R., and Uauy, R. D. (1992) *Invest. Ophthalmol. Vis. Sci.* **33,** 2365–2376
21. McDowell, J. H., and Kuhn, H. (1977) *Biochemistry* **16,** 4054–4060
22. Litman, B. J. (1982) *Methods Enzymol.* **81,** 150–153
23. Jackson, M. L., and Litman, B. J. (1985) *Biochim. Biophys Acta* **812,** 369–376
24. Miller, J. L., Litman, B. J., and Dratz, E. A. (1987) *Biochim. Biophys Acta* **898,** 81–89
25. Fung, B. K., and Stryer, L. (1980) *Proc. Natl. Acad. Sci. U. S. A.* **77,** 2500–2504
26. Bartlett, G. R. (1959) *J. Biol. Chem.* **234,** 596
27. Straume, M., Mitchell, D. C., Miller, J. L., and Litman, B. J. (1990) *Biochemistry* **29,** 9135–9142
28. Thorgeirsson, T. E., Lewis, J. W., Wallace-Williams, S. E., and Kliger, D. S. (1993) *Biochemistry* **32,** 13861–13872
29. Johnson, M., and Frasier, S. (1985) *Methods Enzymol.* **117,** 301–342
30. Niu, S., Mitchell, D. C., and Litman, B. J. (2001) *J. Biol. Chem.* **276,** 42807–42811
31. Mitchell, D. C., Straume, M., Miller, J. L., and Litman, B. J. (1990) *Biochemistry* **29,** 9143–9149
32. Mitchell, D. C., Straume, M., and Litman, B. J. (1992) *Biochemistry* **31,** 662–670
33. Mitchell, D. C., and Litman, B. J. (1998) *Biophys J.* **75,** 896–908
34. Ladha, S., Mackie, A. R., Harvey, L. J., Clark, D. C., Lea, E. J., Brullemans, M., and Duclohier, H. (1996) *Biophys J.* **71,** 1364–1373
35. Borst, J. W., Visser, N. V., Kouptsova, O., and Visser, A. J. (2000) *Biochim. Biophys Acta* **1487,** 61–73
36. Mitchell, D. C., and Litman, B. J. (1998) *Biophys J.* **74,** 879–891
37. Almeida, P. F., Vaz, W. L., and Thompson, T. E. (1992) *Biochemistry* **31,** 6739–6747
38. Boesze-Battaglia, K., Hennessey, T., and Albert, A. D. (1989) *J. Biol. Chem.* **264,** 8151–8155
39. Stinson, A. M., Wiegand, R. D., and Anderson, R. E. (1991) *Exp. Eye Res.* **52,** 218
40. Neuringer, M. (2000) *Am. J. Clin. Nutr.* **71,** 256S–267S
41. Arnis, S., and Hofmann, K. P. (1993) *Proc. Natl. Acad. Sci. U. S. A.* **90,** 7849–7853
42. Jager, S., Szundi, I., Lewis, J. W., Mah, T. L., and Kliger, D. S. (1998) *Biochemistry* **37,** 6998–7005
43. Dickopf, S., Mielke, T., and Heyn, M. P. (1998) *Biochemistry* **37,** 16888–16897
44. Tachibanaki, S., Imai, H., Mizukami, T., Okada, T., Imamoto, Y., Matsuda, T., Fukada, Y., Terakita, A., and Shichida, Y. (1997) *Biochemistry* **36,** 14173–14180
45. Lewis, J. W., Winterle, J. S., Powers, M. A., Kliger, D. S., and Dratz, E. A. (1981) *Photochem. Photobiol.* **34,** 375–384